

Membrane Trapping of Carbon-11-Labeled 1,2-Diacylglycerols as a Basic Concept for Assessing Phosphatidylinositol Turnover in Neurotransmission Process

Yoshio Imahori, Ryou Fujii, Satoshi Ueda, Keigo Matsumoto, Kazuo Wakita, Tatsuo Ido, Tadashi Nariai, and Hisamitsu Nakahashi

Department of Neurosurgery, Kyoto Prefectural University of Medicine, Kyoto, Japan; Nishijin Hospital, Kyoto, Japan; Cyclotron & Radioisotope Center, Tohoku University, Sendai, Japan; and Department of Neurosurgery, Tokyo Medical and Dental University, Tokyo, Japan

The uptake mechanism of 1,2-[¹¹C]diacylglycerols (DAG) was studied and its use as a probe for the measurement of phosphatidylinositol (PI) turnover was verified. A method of synthesis for producing *rac*-1,2-[¹¹C]DAG using [¹¹C]ethylketene was developed to label the 1- or 3-hydroxyl group of 2-monoacylglycerol. After intravenous injection, these tracers were metabolized rapidly in the rat brain cortex to phosphatidic acids, phosphatidylinositols and phosphatidylinositol phosphates. The brain cortex anesthetized by barbiturate, which represents inhibited state of synaptic transmission, did not produce differences in uptake values between *sn*-1,2-[¹¹C]DAG and *rac*-1,2-[¹¹C]DAG. However, in the liver, lung, and pancreas under the same conditions, the uptake values of *rac*-1,2-[¹¹C]DAG were higher than those of *sn*-1,2-[¹¹C]DAG, in which the labeling position was on the 2-hydroxyl group in the *sn* type. These findings suggest that the lipase activity in the brain should be disregarded because lipase predominantly hydrolyzes the 1- or 3-position of *rac*-1,2-[¹¹C]DAG, which should be the main factor producing the differences in uptake values in other organs. Cholinergic stimulation prompted accumulation of 1,2-[¹¹C]DAG in the conscious rat brain. In conclusion, *sn*-1,2-[¹¹C]DAG, administered even in the racemic mixture, could serve as a tracer that becomes mixed with receptor-linked PI turnover and could accumulate in the brain based on the membrane trapping mechanism.

J Nucl Med 1992; 33:413–422

Numerous bioactive agents, which act on the cell surface, manifest their specific cellular functions through regulation of the intracellular reactions via the second messenger system of the target cells (1–3). One example of such a mechanism is neuronal receptor-linked phospha-

tidylinositol (PI) turnover in the central nervous system (CNS). Phospholipase C (PLC), which is associated with receptors, hydrolyzes phosphatidylinositides (PIPs) into *sn*-1,2-diacylglycerol (DAG) and inositolphosphates, promoting the secondary dual turnover system. The PI turnover-protein kinase C (PKC) system is thought to be closely involved in higher cortical functions such as memory and learning (4–6). Therefore, visualization of the *in vivo* PI turnover by positron emission tomography (PET) for the study of CNS function may provide a new approach to human neuroscience.

For visual observation of PI turnover by PET, we synthesized *sn*-1,2-[¹¹C]DAG by ketene reaction (7–9). We previously found high uptake of this tracer in certain regions of the rat brain (e.g., amygdala, cerebral cortex, and hippocampus) (10–12). In that preliminary study, the regions with high neuronal activity, related to PKC (13–15), correspond with those showing high uptake of *sn*-1,2-[¹¹C]DAG. This article mainly describes our recent study with a modified Folch's method (1949) (16) to clarify whether or not the brain uptake of *sn*-1,2-[¹¹C]DAG is due to accumulation of radioactivity based on PI metabolic processes.

This article will additionally refer to *rac*-1,2-[¹¹C]DAG (11). The method for synthesizing *rac*-1,2-[¹¹C]DAG is simpler than that for *sn*-1,2-[¹¹C]DAG. We analyzed the uptake of both *rac*- and *sn*-1,2-[¹¹C]DAG in the rat *in vivo*. The 2-position of glycerol in *sn*-1,2-[¹¹C]DAG was labeled with ¹¹C while the 1-position of glycerol in *rac*-1,2-[¹¹C]DAG was labeled with ¹¹C. The difference in the labeling position between the two isomers should be reflected in different radioactivity uptake between tissues because of tissue-specific metabolic features of ¹¹C butyryl moiety. A condition necessary for DAG to serve as a probe specific to brain PI turnover is that phosphatidic acid (PA) is produced by 1,2-DAG kinase phosphorylation in the initial step of DAG-recycling in PI turnover (1,4) and that a series of polarized components, PI, PIP (phosphatidyl-

Received Apr. 22, 1991; revision accepted Sept. 26, 1991.
For reprints contact: Yoshio Imahori, MD, Department of Neurosurgery, Kyoto Prefectural University of Medicine, Kawaramachi-Hirokoji, Kamigyo 602, Kyoto, Japan.

inositol 4-phosphate), PIP₂ (phosphatidylinositol 4,5-bisphosphate) are produced by subsequent membrane trapping. In this case, *sn*-sterotype is specific to 1,2-DAG kinase (17). Degradation by lipase is also possible (18,19). Lipase predominantly hydrolyzes the 1- and 3-position. In *rac*-1,2-[¹¹C]DAG, it is more likely that the C-11 butyryl moiety is removed by lipase and trapped within the tissue in the form of polarized components. We compared the biodistribution of *sn*- and *rac*-1,2-[¹¹C]DAG and discussed the PI turnover (a metabolic process important for extrinsic 1,2-[¹¹C]DAG) and lipase activity (an additional factor involved) in a rat brain.

MATERIALS AND METHODS

Chemicals

L- α -palmitoyl-lysophosphatidylcholine (1-palmitoyl-*sn*-glycerol-3-phosphorylcholine), L- α -stearoyl lysophosphatidylcholine, 2-palmitoylglycerol, and 2-stearoylglycerol, purchased from Sigma Chemical Co. (St. Louis, MO), as precursors; phospholipase C, Type III from *Bacillus cereus* (Lecithinase C; EC 3.1.4.3), purchased from Wako Pure Chemicals Industries (Osaka); arecoline hydrobromide, purchased from Research Biochemicals (Natick, MA), and butyl scopolamine bromide, purchased from Sigma Chemical Co.

Ketene Method

The procedure is as described in our previous report (9,12,20, 21). Carbon-11-labeled carbon dioxide was produced by a ¹⁴N(p, α)¹¹C reaction using a cyclotron (The Japan Steel Works, model BC1710) and automated synthesis system for producing [¹¹C]ethylketene was used (The Japan Steel Works, the prototype of ¹¹C-ketene system). Carbon-11-ethylketene was trapped directly in the pyridine solution containing a precursor. All of the acylation

reactions were performed under no-carrier added conditions at room temperature and within 5 min.

Synthesis of 1-palmitoyl-2-[1-¹¹C]butyryl-*sn*-glycerol

As shown in Figure 1, 1 μ mol of L- α -palmitoyl-lysophosphatidylcholine (1) was used as a precursor. L- α -palmitoyl-2-[1-¹¹C]-butyryl-*sn*-glycerol-3-phosphorylcholine (2) was obtained as an [¹¹C]ethylketene adduct. To remove the phosphorylcholine by an enzymatic reaction modified from that used by Zwaal et al. (22, 23), phospholipase C (PLC; 5 U, Type III from *Bacillus cereus*) (24) was employed. 1-palmitoyl-2-[1-¹¹C]butyryl-*sn*-glycerol (3) was obtained in the ether phase (12).

Synthesis of 1-[1-¹¹C]butyryl-2-palmitoyl-*rac*-glycerol

Carbon-11-ethylketene was induced to react in 300 μ l of pyridine containing 1 μ mol of 2-palmitoylglycerol (4) in Figure 1 and 0.5 μ mol of DMAP at room temperature for 5 min. Then, unreacted [¹¹C]ethylketene and pyridine were completely removed using an evaporator. 1-[1-¹¹C]butyryl-2-palmitoyl-*rac*-glycerol (5) was verified by the HPLC system with the standard material.

Synthesis of 1-[1-¹¹C]butyryl-*rac*-glycerol

This monoacylglycerol (MAG) tracer was employed for comparison with 1,2-[¹¹C]DAG, since MAG is a good substrate for lipase but not for DAG kinase. [¹¹C]ethylketene was induced to react in 300 μ l of pyridine containing 1 μ mol of glycerol (6) in Figure 1 and 0.5 μ mol of DMAP and the other procedures were the same as above. 1-[1-¹¹C]butyryl-*rac*-glycerol (7) was verified by the HPLC system with the standard material.

sn-1,2- and *rac*-1,2-[¹¹C]DAG Metabolic Studies by Modified Folch's Method

A 150-mg portion of rat cerebral cortex was removed from a rat brain (male Wistar rats weighing 300 g) administered with a dose of 1.5–8 mCi of [¹¹C]DAG, dissolved in 0.4 ml saline with

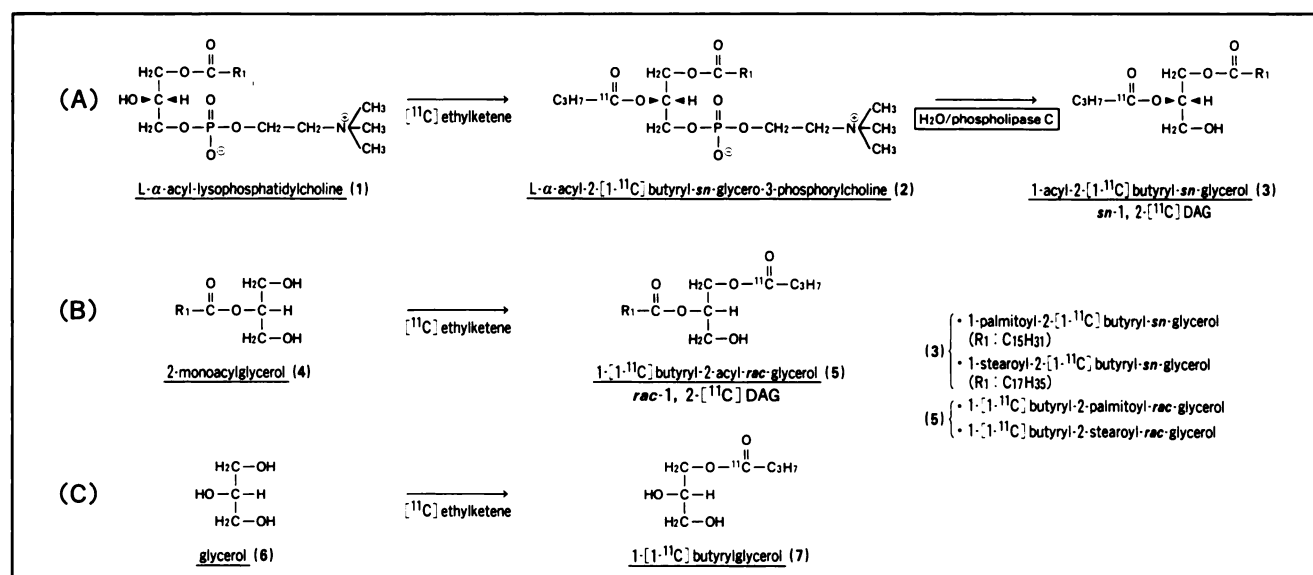


FIGURE 1. Synthesis of no-carrier-added *sn*- and *rac*-1,2-[¹¹C]DAGs and 1-[¹¹C]butyryl-*rac*-glycerol by the ketene method. (A) Synthesis of 1-acyl-2-[¹¹C]butyryl-*sn*-glycerol (*sn*-1,2-[¹¹C]DAG). This reaction consists of two main procedures: ethylketene reaction and PLC hydrolysis (12). (B) Synthesis of 1-[¹¹C]butyryl-2-palmitoyl-*rac*-glycerol. (*rac*-1,2-[¹¹C]DAG). The main procedure was an acylation to the 1- or 3-hydroxyl group of 2-acylglycerol by ethylketene reaction. (C) Synthesis of 1-[¹¹C]butyryl-*rac*-glycerol. (*rac*-1-[¹¹C]MAG). The main procedure was the same as (B). The radio-HPLC profiles are shown in Figure 2.

0.1% bovine serum albumin and 0.5% DMSO at 5 and 20 min after injection of [¹¹C]DAG. Three kinds of lipid solvent were used to extract brain phospholipids. The tissue was homogenized for 3 min by grinding manually with about 0.5 ml of the solvent (chloroform/methanol; 3/2, v/v) and was centrifuged at 3000 rpm (1660 g, Kubota KR/702) at 10°C for 3 min. Two phases were observed with a pellet positioned between the water phase and chloroform phase. Both phases were collected together and the pellet was re-homogenized with 0.5 ml of the second solvent (chloroform/methanol/water; 1/2/0.3, v/v) and was centrifuged in 3000 rpm for 3 min. The supernatant was added to the soluble fraction and a pellet was re-homogenized with 0.5 ml of the third solvent (methanol/water; 2/3, v/v). The supernatant was also added to the soluble fraction. Then 0.5 ml of chloroform and 0.5 ml of water were newly added to the soluble fraction and the mixture was shaken. The chloroform and water-phase mixtures were separated. Total time was about 40 min until the final extraction. The extracted lipids of both samples were spotted on TLC plates, Silica Gel 60 (activated).

Thin-Layer Chromatography

We employed two solvent systems of mobile phase and Silica Gel 60 (activated) as a stationary phase for analysis of ¹¹C-labeled phosphoinositides (PI, PIP, and PIP₂) in the extraction and 1,2-[¹¹C]DAG was separated from the polarized component in the serum. The two solvent systems consisted of neutral and basic polar solvents, system (A); chloroform/methanol/water:65/25/4, v/v, and system (B); chloroform/methanol/20% methylamine: 60/36/10, v/v (25). The plates (length 75 mm) were developed in one dimension in each solvent system. The developed TLC was put into contact with an imaging plate of Fuji Computed Radiography System (FCR) which was exposed for 1 hr and then calculated to obtain digitalized images. The positions of the various phospholipid radioactivities were visualized by FCR system and were identified by comparison with the authentic compounds. The PA, PI, PIP, PIP₂, and along with other phospholipids and their authentic compounds were visualized with common lipid locating agents such as I₂ or molybdenum blue spray for phosphate on the same TLC plates.

Degradation of the Extrinsic Added 1,2-[¹¹C]DAG in Rat Serum

The degradation of 1-[¹¹C]butyryl-2-palmitoyl-rac-glycerol was studied in rat serum (male Wistar rats each weighing 300 g to 305 g). A dose of 3 mCi was injected (within 3 sec) through the tail vein. Time sequence blood samples (300 µl) were collected at 0, 2.5, 5, 7, 10, and 20 min, making a total of six samples in a period of 20 min. The serum was then spotted on TLC plates as described in the former section.

Biodistribution of sn- and rac-1,2-[¹¹C]DAG Under a Deeply Anesthetized Condition and a Conscious Condition

Tracer distribution in rats (male Wistar rats each weighing 300 g to 305 g) was measured by the following procedure. A dose of 0.8–3 mCi of [¹¹C]DAG dissolved in 0.4 ml saline with 0.1% bovine serum albumin and 0.5% DMSO was injected in three experimental groups; 1-palmitoyl-2-[¹¹C]butyryl-sn-glycerol in the deeply anesthetized group (n = 3), 1-[¹¹C]butyryl-2-palmitoyl-rac-glycerol in the deeply anesthetized group (n = 4), and 1-

[1-¹¹C]butyryl-2-palmitoyl-rac-glycerol in the conscious group (n = 4). Both tracers were administered through the tail vein under an anesthetized condition with 45 mg/kg of sodium pentobarbital (in deeply anesthetized groups) and under transiently anesthetized conditions induced by halothane (0.7%) in room air in the conscious group. An intravenous bolus injection of each ¹¹C-DAG was given, and 30 min later the rats were killed by decapitation. The brains were rapidly removed and divided into cortex and cerebellum and other organs, such as the liver, lung, heart and pancreas, were also removed. Tissue radioactivity was measured using a gamma counter and the tissue samples were weighed. Uptake was expressed as %dose/g; (count/g tissue) × (1/total injected count) × 100%. The data obtained in triplicate (sn-1,2-[¹¹C]DAG) and quadruplicate (rac-1,2-[¹¹C]DAG) experiments were presented as average ± s.d.

Exhaust of ¹¹CO₂ to Expiration on sn- and rac-1,2-[¹¹C]DAG Injection

These experiments were performed along with biodistribution studies as described above in the study of 1-palmitoyl-2-[¹¹C]-butyryl-sn-glycerol under deep anesthesia (n = 3) and in the study of 1-[¹¹C]butyryl-2-palmitoyl-rac-glycerol under deep anesthesia (n = 4). ¹¹CO₂ was continuously collected into each soda-lime column for 5-min periods, for a total of six periods and 30 min. The column radioactivity was measured using a gamma counter.

Cholinergic Stimulation Study in Conscious Rat Brain

Cholinergic stimulation studies were performed by the administration of arecoline under the condition of systemic cholinergic blockage (26) by using butylscopolamine bromide. A rat (male Wistar rat weighing 300–305 g) was administered saline with butylscopolamine bromide (6.6 mg/kg; s.c.) 20 min prior to an i.p. administration of saline (control: n = 4) or arecoline (13 mg/kg; n = 4). Five minutes after arecoline injection, 3 mCi of 1-[¹¹C]-butyryl-2-palmitoyl-rac-glycerol were injected into a tail vein. At 30 min after tracer injection, the rat was killed with sodium pentobarbital (5 g/kg, i.v.). The brain was rapidly removed and regional brain tissue radioactivities (cerebral cortex and cerebellum) and blood radioactivity were measured using a gamma counter and tissue samples were weighed as described above.

The Performance of the Coincidental Gamma Counter-Rat Brain Monitoring System

The radioactivity in the rat brain was monitored by a pair of external coincidence BGO detectors. The detector pair was positioned to detect radioactivity in a brain, with minimum contaminating signals from the extracerebral tissue, using 3-mm diameter zones marked on the exposed skull of the animals. We obtained a time-activity curve of 1-[¹¹C]butyryl-2-palmitoyl-rac-glycerol, in distinct contradiction to 1-[¹¹C]butyryl-rac-glycerol as MAG. Each tracer was injected in bolus administration (within 3 sec) through the tail vein. Time sequence counting was done by the timing single-channel analyzer connected to a computer (PC 9801; NEC). Data were collected continuously in 3-min periods, for a total of 12 periods totaling 36 min. The ability to isolate counts from 3 mm zones indicated an FWHM of 3.2 mm. The scattering ratios of each measurement in a 3-min period were from 5.4% s.d. in 200 counts to 1.7% s.d. in 2000 counts.

TABLE 1
Synthesis of ^{11}C -Labeled DAGs and MAG

Synthesis time	yield*	purity†	Specific activity
$[^{11}\text{C}]$ ethylketene			
L- α -palmitoyl-2-[1- ^{11}C]butyryl-sn-glycero-3-phosphorylcholine (2) 30 min (5 min [§])	— 25%	— 75%	186-279GBq/ μmol [‡] 186GBq/ μmol (5Ci/ μmol)
1-palmitoyl-2-[1- ^{11}C]butyryl-sn-glycerol (3) 50 min	4%	96%	93GBq/ μmol (2.5Ci/ μmol)
1-[1- ^{11}C]butyryl-2-palmitoyl-rac-glycerol (5) 30 min	35%	96%	186GBq/ μmol (5Ci/ μmol)
1-[1- ^{11}C]butyryl-rac-glycerol (7) 30 min	35%	96%	186GBq/ μmol (5Ci/ μmol)

* Calculated from the trapped $^{11}\text{CO}_2$.

† Based on radio-HPLC profile obtained before the process of separative HPLC.

‡ Estimating specific activity of $[^{11}\text{C}]$ ethylketene by using 12-deoxyphorbol 13-isobutyrate 20-[1- ^{11}C]butyrate as an indicator (12).

[§] as the $[^{11}\text{C}]$ ethylketene adduct and not to be separated. Numbers in parentheses are each compound as mentioned in Figure 1.

RESULTS

Synthesis of ^{11}C -Labeled DAGs

Table 1 shows the radiochemical yield, purity, specific activity, and total synthesis time of 1-palmitoyl-2-[1- ^{11}C]butyryl-sn-glycerol (3), 1-[1- ^{11}C]butyryl-2-palmitoyl-rac-glycerol (5), and 1-[1- ^{11}C]butyryl-rac-glycerol (7). The specific activity of these $[^{11}\text{C}]$ ethylketene adducts was about 186 GBq/ μmol (5 Ci/ μmol) at the end of synthesis. The hydrolyzing ratio of $[^{11}\text{C}]$ ethylketene adduct in PLC reaction was about 15% for the production of 1-palmitoyl-2-[1- ^{11}C]butyryl-sn-glycerol (12). The ^{11}C adduct of 2-palmitoylglycerol is rac-1,2-[^{11}C]DAG in the no-carrier-added reaction, which was an acylation to the 1- or 3-hydroxyl group (Fig. 2A). 1-[1- ^{11}C]butyryl-rac-glycerol is obtained

in the no-carrier-added reaction which was the same reaction to glycerol by $[^{11}\text{C}]$ ethylketene (Fig. 2B).

sn-1,2-[^{11}C]DAG Metabolic Fates by Using Folch's Method: Extraction of Phosphoinositides

Lipid extraction was done without using acidified solvent to avoid the deacylation of phosphatidylinositols. Almost all radioactivity in the brain was extracted due to the presence of water in the sample. Approximately 15% of the total radioactivity was in the CHCl₃-rich organic phase, 80% was in the water phase, and 5% was in the interfacial precipitate. Both phases included crude polyphosphoinositides, which can be further separated to yield individual PIPs by TLC.

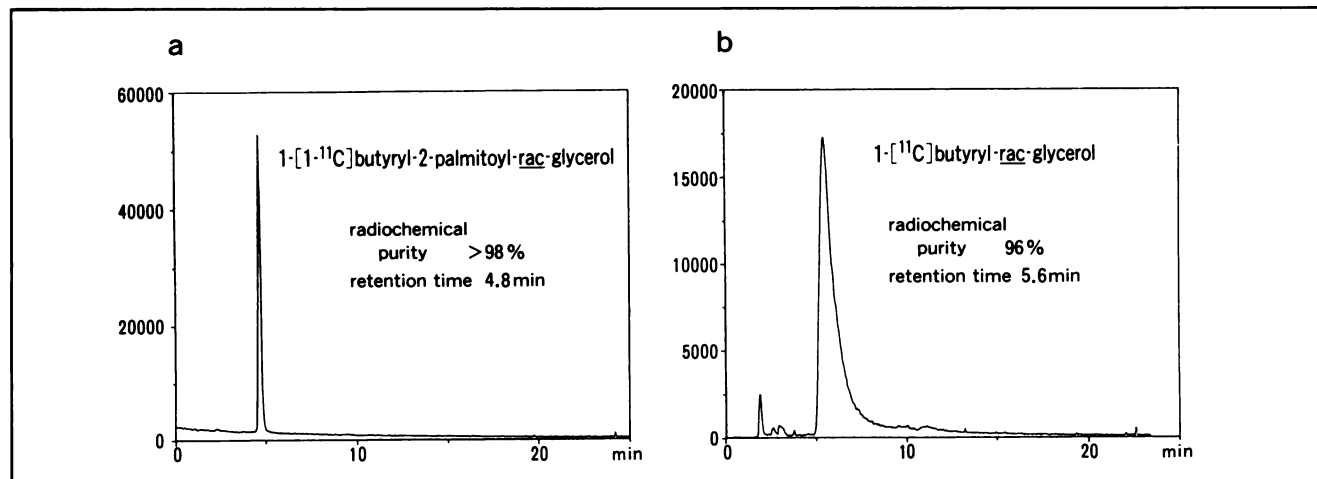


FIGURE 2. Radio-HPLC profiles of 1-[1- ^{11}C]butyryl-2-palmitoyl-rac-glycerol (A) and 1-[1- ^{11}C]butyryl-rac-glycerol (B). All diacylglycerols were analyzed by HPLC and UV spectra were measured in hexane in 1 cm cells in a sequential connected spectrophotometer (Shimadzu model SPD-6AV) by using 242 nm in UV wave length. Zorbax SIL (Dupont Instrument, 4.6 mm \times 25 cm) was used. The HPLC was operated at room temperature. DAGs (a) and MAGs (b) were separated by using hexane/isopropyl alcohol (95:5, v/v) and hexane/ether/isopropyl alcohol (10:2:1, v/v), respectively. The flow rate was 1.8 ml/min. The radioactivity included in the eluent was sequentially counted by using multi-channel analyzer. X-axis, a channel number of radio-HPLC (3 sec/channel). Y-axis, each channel radioactivity of tracer.

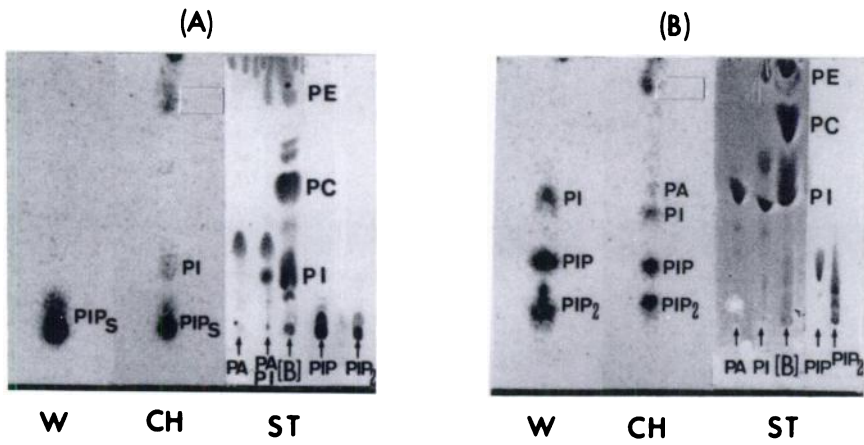


FIGURE 3. Radio-TLC profiles of ^{11}C -labeled PI turnover intermediates. The brain extracts were obtained 20 min after $1-[1-^{11}\text{C}]$ butyryl-2-palmitoyl-rac-glycerol injection. The total injected dose was 8 mCi per rat (300 g) in this case. TLC (Silica Gel 60, activated, as a stationary phase) for analysis of ^{11}C -labeled phosphoinositides (PI, PIP, and PIP_2) in the extraction by modified Folch's method. System (A), chloroform/methanol/water: 65/25/4, v/v. System (B), chloroform/methanol/20% methylamine: 60/36/10, v/v. W = Radio-TLC of the water fraction; CH = Radio-TLC of the chloroform fraction; ST = TLC of the lipids from brain ([B]) and standards (PA, PI, PIP, PIP_2) visualized by I_2 .

As shown in Figure 3, the positions of the various phospholipid radioactivities were visualized by the FCR system and were identified by standards in two different developing systems, (A) and (B). The 1,2- $[^{11}\text{C}]$ DAG metabolites, PA, PI, PIP, PIP_2 , and their standards were visualized on the same TLC plates. Figure 3 shows a typical pattern for the brain extracts 20 min after *rac*-1,2- $[^{11}\text{C}]$ DAG injection. A similar TLC pattern was obtained for *sn*-1,2- $[^{11}\text{C}]$ DAG and *rac*-1,2- $[^{11}\text{C}]$ DAG 5 min after injection. The unmetabolized *sn*- or *rac*-1,2- $[^{11}\text{C}]$ DAG was observed concomitant with the PI intermediates at 5 min after injection; however, it merged gradually into PI intermediates. By 20 min after administration, almost all of the DAG had been metabolized into the PI intermediates.

Degradation of the Extrinsic Added 1,2- $[^{11}\text{C}]$ DAG in Rat Serum

Figure 4 shows the TLC profiles. Degradation of $1-[1-^{11}\text{C}]$ butyryl-2-palmitoyl-rac-glycerol occurred rapidly in the rat serum. The blood radioactivity values (whole blood) were $0.25 \pm 0.02\% \text{dose/g}$ and $0.17 \pm 0.03\% \text{dose/g}$ at 10 min and 30 min after injection in a time course, respectively. However, almost all of the 1,2- $[^{11}\text{C}]$ DAG had dis-

appeared by 10 min. The 1,2- $[^{11}\text{C}]$ DAG practically persisted for only initial several minutes in the blood.

Biodistribution of *sn*-1,2- and *rac*-1,2- $[^{11}\text{C}]$ DAG

Biodistribution of 1-palmitoyl-2-[1- ^{11}C]butyryl-*sn*-glycerol ($n = 3$) and 1-[1- ^{11}C]butyryl-2-palmitoyl-*rac*-glycerol ($n = 4$) was investigated 30 min after injection of each tracer. No differences between *sn*-1,2- and *rac*-1,2- $[^{11}\text{C}]$ DAG values were seen in the cerebral cortex, cerebellum, and blood under a deeply anesthetized condition (Fig. 5a-b), and large differences were seen in the liver, pancreas, and lung (Table 2). More *rac*-1,2- $[^{11}\text{C}]$ DAG than *sn*-1,2- $[^{11}\text{C}]$ DAG was accumulated in the liver, pancreas, and lung; but the reverse occurred in the kidney and urine. Regional variations may be attributed to regional biochemical events.

In Table 3, the *rac*-1,2- $[^{11}\text{C}]$ DAG uptake in the conscious group ($n = 4$) was compared with that in the deeply anesthetized group (Table 2). In the conscious state (Fig. 5c-d), 1,2- $[^{11}\text{C}]$ DAG uptake in the cortex was slightly increased, but that in the blood was decreased ($0.001 < p < 0.01$). Therefore, brain/blood ratios showed an increase in the conscious state.

Exhaust of $^{11}\text{CO}_2$ to Expiration After *sn*- and *rac*-1,2- $[^{11}\text{C}]$ DAG Injection

Both studies on the 1-palmitoyl-2-[1- ^{11}C]butyryl-*sn*-glycerol group ($n = 3$) and 1-[1- ^{11}C]butyryl-2-palmitoyl-*rac*-glycerol group ($n = 4$) in the deeply anesthetized condition demonstrated a continuous expiration profile of $^{11}\text{CO}_2$ during the 30-min period study (Fig. 6). This suggested that $^{11}\text{CO}_2$ expiration accurately reflects the deacylation process from the 1-position of 1,2- $[^{11}\text{C}]$ DAG by lipase and further process of β -oxidation via [1- ^{11}C]butyryl CoA. The cumulative expiration radioactivity values of *sn*- and *rac*-1,2- $[^{11}\text{C}]$ DAG were 9.5 ± 1.3 and $11.4 \pm 2.4\% \text{dose/total injected dose}$, respectively ($0.3 < p < 0.5$).

Cholinergic Stimulation Study Using Conscious Rat Brain

Regional brain uptake of $1-[1-^{11}\text{C}]$ butyryl-2-palmitoyl-*rac*-glycerol was investigated 30 min after injection. Large

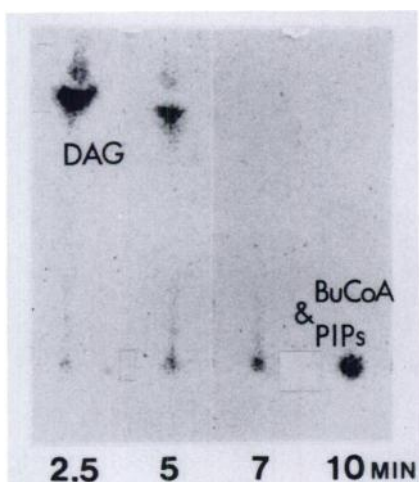


FIGURE 4. The degradation of the extrinsic added 1,2- $[^{11}\text{C}]$ DAG in a rat serum. The time course of degradation of $1-[1-^{11}\text{C}]$ butyryl-2-palmitoyl-rac-glycerol in rat serum. The total Injected Dose was 3 mCi per rat. TLC development solvent was employed system (A) described in Figure 3.

TABLE 2
Biodistribution of *sn*-1,2- and *rac*-1,2-[¹¹C]DAGs in Deeply Anesthetized Condition 30 Minutes After Injection

	1-palmitoyl 2-[¹¹ C]butyryl- <i>sn</i> -glycerol (N = 3) [†]	1-[1- ¹¹ C]butyryl 2- palmitoyl- <i>rac</i> - glycerol (N = 4) [‡]	t-test*
	mean ± s.d. (%dose/g)	mean ± s.d. (%dose/g)	
Cerebral cortex	0.116 ± 0.014	0.116 ± 0.012	0.5 < p < 1 ns
Cerebellum	0.110 ± 0.024	0.113 ± 0.015	0.5 < p < 1 ns
Temporal muscle	0.090 ± 0.005	0.076 ± 0.007	0.02 < p < 0.05
Heart	0.126 ± 0.023	0.147 ± 0.010	0.2 < p < 0.3
Pancreas	0.176 ± 0.031	0.311 ± 0.053	0.001 < p < 0.01
Lung	0.422 ± 0.076	0.630 ± 0.136	0.05 < p < 0.1
Liver	0.341 ± 0.026	0.628 ± 0.067	0 < p < 0.001
Kidney	0.457 ± 0.038	0.270 ± 0.008	0 < p < 0.001
Urine	8.96 ± 0.178	1.14 ± 0.627	0 < p < 0.001
Blood	0.166 ± 0.027	0.164 ± 0.011	0.5 < p < 1 ns

* For comparison between the *sn*-1,2-[¹¹C]DAG and *rac*-1,2-[¹¹C]DAG by t-test. ns = not significant.

† The total injected dose was 0.8 mCi per rat.

‡ The total injected dose was 1.6 mCi per rat.

Biodistribution studies were performed using male Wistar rats each weighing 300–350 g under a deeply anesthetized condition (45 mg/kg). Carbon-11-labeled DAGs were injected through a tail vein. The rats were killed 30 min postinjection. Tissue uptake was expressed as %dose/g. Data present average ± s.d. in triplicate or quadruplicate experiments.

differences between the control group (n = 4) and cholinergic stimulated group (n = 4) were seen in the cerebral cortex (p < 0.01) and cerebellum (p < 0.001), and no significant differences were seen in the blood (p > 0.3) (Table 4). The 1,2-[¹¹C]DAG uptake values in the cortex and cerebellum showed an increase of 26% and 34%, respectively. This shows that the uptake of 1,2-[¹¹C]DAG was enhanced by cholinergic stimulation. These findings suggested that 1,2-[¹¹C]DAG uptake is related to receptor-linked PI turnover in the brain.

Time-Activity Curves of ¹¹C-DAG and ¹¹C-MAG in Rat Brain Using a Coincidental Gamma Counter System

Biodistribution study using 1-[1-¹¹C]butyryl-2-palmitoyl-*rac*-glycerol with a time course suggested a tracer accumulation in the brain (Table 5).

Two time-activity curves of 1-[1-¹¹C]butyryl-2-palmitoyl-*rac*-glycerol and 1-[1-¹¹C]butyryl-*rac*-glycerol were obtained as shown in Figure 7. The former showed accumulation and the latter showed disappearance. These findings suggest that 1,2-[¹¹C]DAG can be metabolized into

TABLE 3
Comparison of 1-[1-¹¹C]butyryl-2-palmitoyl-*rac*-glycerol Tissue Uptake in Conscious Group (n = 4) with the Deeply Anesthetized Group (n = 4, in Table 1)

	Conscious state (n = 4) mean ± s.d. (%dose/g) [†]	t-test*	Variations
Cerebral cortex	0.128 ± 0.007	0.1 < p < 0.2	↑
Cerebellum	0.108 ± 0.006	0.5 < p < 1	ns
Temporal muscle	0.075 ± 0.004	0.5 < p < 1	ns
Heart	0.126 ± 0.005	0.01 < p < 0.02	↓
Pancreas	0.240 ± 0.039	0.05 < p < 0.1	↓
Lung	0.432 ± 0.179	0.1 < p < 0.2	↓
Liver	0.613 ± 0.056	0.5 < p < 1	ns
Kidney	0.305 ± 0.029	0.05 < p < 0.1	↑
Urine	1.81 ± 0.583	0.2 < p < 0.3	↑
Blood	0.136 ± 0.007	0.001 < p < 0.01	↓

* For comparison between the deeply anesthetized group (n = 4, on the third column in Table 2). ns = not significant.

† The total injected dose was 1.6 mCi per rat.

A variation in the 1-[1-¹¹C]butyryl-2-palmitoyl-*rac*-glycerol uptake between the two groups was observed. Light anesthesia using halothane was used during the short period (3 min) for tracer administration in the conscious group. Tissue distribution was examined using male Wistar rats each weighing 300–305 g. 1-[1-¹¹C]butyryl-2-palmitoyl-*rac*-glycerol was injected through a tail vein. The rats were killed 30 min after the injection. The regional uptake was expressed as %dose/g. Data present average ± s.d. (n = 4).

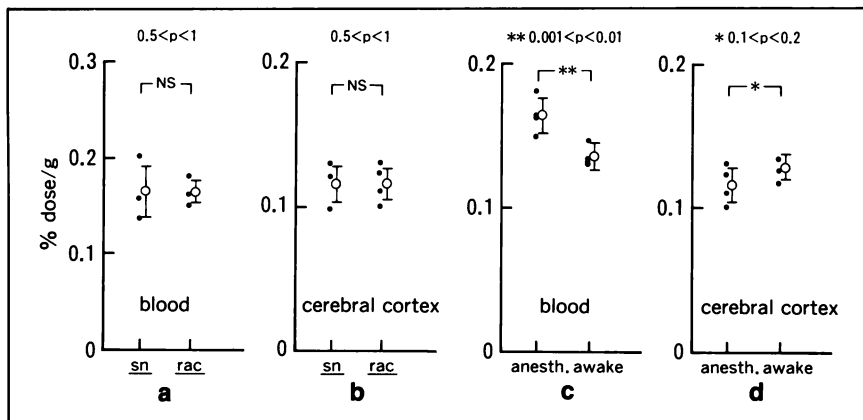


FIGURE 5. Biodistribution of *sn*- and *rac*-1,2-[¹¹C]DAG under the deep anesthetized condition and the conscious condition. (I) A comparison of 1-palmitoyl-2-[1-¹¹C]butyryl-*sn*-glycerol group (*n* = 3) with 1-[1-¹¹C]butyryl-2-palmitoyl-*rac*-glycerol (*n* = 4) under the same deep anesthetic condition in blood (a) and in the cerebral cortex (b). (II) A comparison of deeply anesthetized group with conscious group both using 1-[1-¹¹C]butyryl-2-palmitoyl-*rac*-glycerol in blood (c) and in the cerebral cortex (d).

polarized compounds, which can be trapped in the cell membrane. This assumption is supported by the findings obtained using the TLC study (Fig. 3). On the contrary, 1-[1-¹¹C]butyryl-*rac*-glycerol cannot be trapped in the brain, which suggests that the *rac*-1-[¹¹C]MAG cannot be metabolized into [1-¹¹C]butyryl CoA due to the lack of lipase activity in the rat brain.

DISCUSSION

A basic method for the visualization of intracellular signaling, employing extrinsic added 1,2-[¹¹C]DAG, which can be applied to PET imaging is reported. The theoretical background for this study is the PI turnover which was systematically studied by Berridge et al. (1984). In this dual-second messenger system, *sn*-1,2-DAG appears fol-

lowing neuronal signaling but is soon metabolized by 1,2-DAG kinase into PA under normal neuronal activity. After this step in PI turnover, functional lipids (PI, PIP, and PIP₂) are formed via CDP-DAG and coexist in the cell membrane together with structural lipids such as phosphatidylcholine (PC) and phosphatidylethanolamine (PE). Figure 8 summarizes PI turnover, 1,2-DAG is cell-permeable and can pass through the blood-brain barrier (BBB) (27,28). This property of 1,2-DAG allows it to serve as a convenient tracer of PI turnover. The administered 1,2-[¹¹C]DAG was metabolized into PA, PI, PIP, and PIP₂ within 5 min after injection, while radioactive PC and PE did not appear even after 20 min (Fig. 3). This indicates negligible transacylation of the acyl residue of ¹¹C-labeled PIPs into other structural lipids. In other words, intravenously administered extrinsic *sn*-1,2-[¹¹C]DAG rapidly traces the course of PI turnover as shown in Figure 8. In this connection, we propose a concept of membrane trapping, that is PIP accumulation in the membrane, to explain the above-mentioned trapping mechanism, because the possibility of re-mobilization of ¹¹C-labeled PIPs after incorporation into a cell membrane seems to be very low. As shown in Figure 7, time-activity curve analysis with a coincidental gamma counter demonstrated a *rac*-1,2-[¹¹C]-DAG accumulation pattern in the brain. This finding supported the view that membrane trapping occurs *in vivo* because of the presence of *sn*-type in a racemic mixture.

Another important possibility is that the administration of *sn*- or *rac*-1,2-[¹¹C]DAG is degraded by lipase in the brain or other organs (e.g., liver, pancreas) involved in the systemic circulation (29). As shown in the results section, about 10% of the total activity was eliminated into expired gas in the continuous form of ¹¹CO₂ within 30 min after tracer injection (Fig. 6). This suggests a metabolic pathway where free fatty acid (FFA), released from 1,2-DAG by lipase, undergoes beta-oxidation to become acetyl CoA.

A major problem in this kind of study is that the metabolic rate of 1,2-DAG based on the lipase activity needs to be much lower than the metabolic rate based on PI turnover. As previously described, lipase from these organs can hydrolyze the 1- and/or 3-position of triglyc-

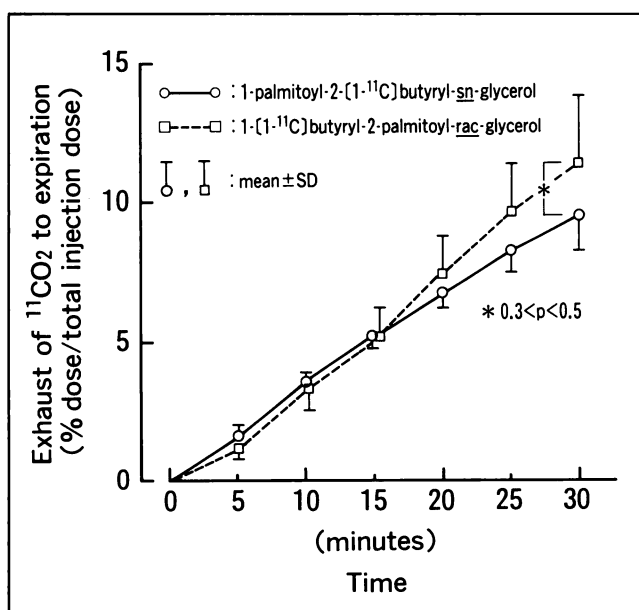


FIGURE 6. ¹¹CO₂ expiration of *sn*- and *rac*-1,2-[¹¹C]DAG. Carbon-11 labeled carbon dioxide, which was produced from the total expiration of rats under enclosed condition separated from the air, was continuously collected into each soda lime column for 5-min periods, making a total of 6 periods for 30 min.

TABLE 4
Cholinergic Stimulation Study of 1-[1-¹¹C]butyryl-2-palmitoyl-rac-glycerol with Arecoline (Intraperitoneal Injection)

	Control (n = 4) mean ± s.d. (%dose/g) [†] (minimum-maximum)	Arecoline-stimulated (n = 4) mean ± s.d. (%dose/g) [†] (minimum-maximum)	t-test*
Blood	0.223 ± 0.016 (0.208 – 0.249)	0.234 ± 0.014 (0.212 – 0.247)	0.3 < p < 0.5 ns
Cerebral cortex	0.182 ± 0.018 (0.160 – 0.206)	0.229 ± 0.015 (0.214 – 0.249)	0.001 < p < 0.01
Cerebellum	0.152 ± 0.014 (0.131 – 0.165)	0.203 ± 0.011 (0.192 – 0.218)	0 < p < 0.001

* For comparison between the control group (n = 4) and arecoline-stimulated group (n = 4) by t-test. ns = not significant.
[†] The total injected dose was 3 mCi per rat.

Effect of cholinergic stimulation on 1-[1-¹¹C]butyryl 2-palmitoyl-rac-glycerol uptake in the brain was examined by arecoline i.p. injection. This procedure of cholinergic stimulation was described in detail in the method section. The rats were killed 30 min after injection. Regional uptake was expressed as %dose/g. Data present average ± s.d. (n = 4).

erides, DAGs, and MAGs to yield polarized components (18). As shown in the results section, the uptake of rac-1,2-DAG labeled at the 1-position was significantly higher than that of sn-1,2-DAG labeled at 2-position in the liver and pancreas (Table 2). This suggests the involvement of lipase in these organs. In the brain, on the contrary, no significant difference was noted between the uptake of sn- and rac-1,2-DAG with different ¹¹C labeling positions (Fig. 5b), which suggests that lipase activity is extremely low in the brain. Under deep pentobarbital anesthesia, synaptic transmission in the brain can be regarded to be in an inhibited state (30) so that the state may not produce any differences based on the PI response in synapse. Additionally, 1-[1-¹¹C]butyryl-rac-glycerol cannot be trapped in the brain (Fig. 7), which suggests that 1-[¹¹C]MAG cannot be metabolized into [1-¹¹C]butyryl CoA because monoacyl glycerol can be readily degraded by monoacyl glycerol

lipase (18,29). These findings suggest that lipase activity in the brain should be disregarded.

In a conscious state, the uptake was increased by about 30% in the presence of cholinergic stimulation (Table 4), which is in agreement with the findings obtained by another method (31,32). These findings suggest that brain rac-1,2-[¹¹C]DAG uptake is closely related to the metabolism via PI turnover. Comparison of the spots on the TLC of rat brain extracts with those of authentic compounds, revealed that the metabolites are PI turnover specific and

TABLE 5
Biodistribution in the Brain with a Time Course Using 1-[1-¹¹C]butyryl-2-palmitoyl-rac-glycerol*

Whole blood (n = 4) mean ± s.d. (%dose/g)	Cerebral cortex (n = 4) mean ± s.d. (%dose/g)
30 sec 0.58 ± 0.05	0.08 ± 0.02
5 min 0.33 ± 0.04	0.10 ± 0.02
10 min 0.25 ± 0.02	0.13 ± 0.03
20 min 0.18 ± 0.02	0.12 ± 0.01
30 min 0.17 ± 0.03	0.12 ± 0.01

* The total injected dose was 1.6 mCi per rat.

Light anesthesia using halothane was used during the short period for tracer administration in the conscious rat. Tissue distribution (especially in the cerebral cortex and blood) was examined using male Wistar rats each weighing 300–305g. 1-[1-¹¹C]butyryl 2-palmitoyl-rac-glycerol was injected through a tail vein. The rats were killed each time after the injection. The brain uptake was expressed as %dose/g. Data present average ± s.d. (n = 4).

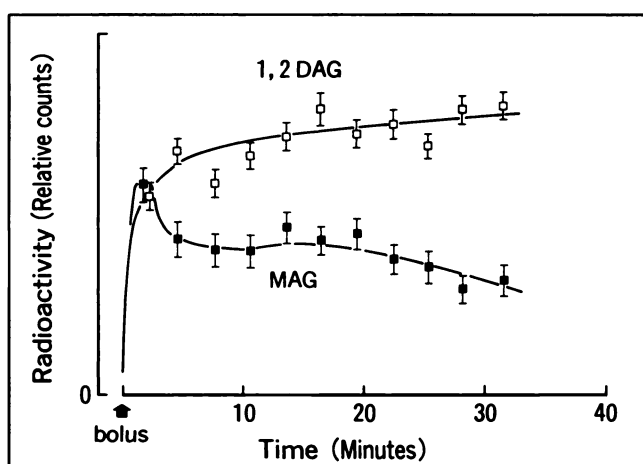


FIGURE 7. Time-activity curves of rac-1,2-[¹¹C]DAG and rac-1-[¹¹C]MAG by using coincidental γ -counter in a rat brain. The radioactivity in rat brain was monitored by a pair of external coincidence BGO detectors. Each tracer was injected in bolus administration (within 3 sec) through tail vein. Data was collected continuously for 3-min periods, making a total of 12 periods for 36 min. Both data were transformed by the relative counts which was consistent with each count at the initial period (from 0 min to 3 min) after bolus injection. Similar time-activity curves were obtained in three experiments in each group. * = open square in rac-1,2-[¹¹C]DAG and close square in rac-1-[¹¹C]MAG; vertical rods are each 1 s.d.

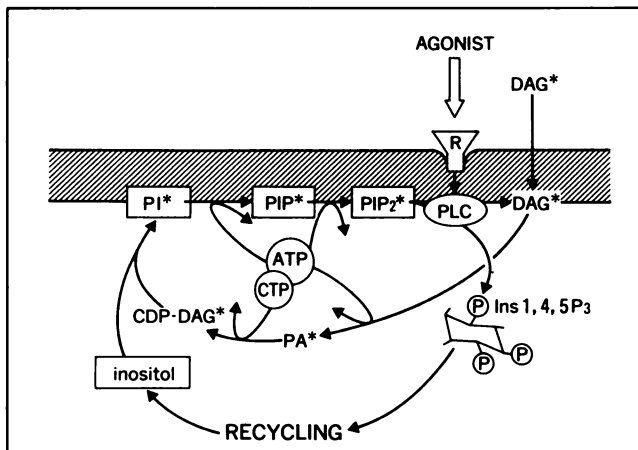


FIGURE 8. "Membrane Trapping" mechanism of extrinsic added 1,2-[¹¹C]DAG. * is ¹¹C-labeled compound and intermediates in PI turnover.

represent rapid metabolism. Transacylation into structural lipids occurred only in very small amounts (Fig. 3), while metabolism in blood occurred rapidly with polarized components being produced in about 5 min after administration. *rac*-1,2-[¹¹C]DAG disappeared from the blood within 10 min and was completely altered to the polarized component (Fig. 4). Once polarized, *sn*- or *rac*-1,2-[¹¹C]DAG cannot pass through the BBB and does not affect its uptake in the brain where its accumulation has already occurred. However, the ¹¹C-labeled metabolized component in serum has to be deduced from the total serum activity, representing the real input function.

Figure 9 summarizes the metabolic fates of each tracer in two modes, PI turnover and lipase deacylation of the [1-¹¹C]butyryl moiety. The metabolic fate of 1,2-[¹¹C]DAG

is predominantly subjected to the course of PI turnover in the brain and the tracer leftover could return to the serum. However, in other organs, such as the liver and pancreas, degradation by lipase is the main course, producing a difference between the accumulation of both tracers. In the case of 1-palmitoyl-2-[1-¹¹C]butyryl-*sn*-glycerol, the 2-position of glycerol was labeled with C-11; however, lipase predominantly hydrolyzes the 1-position (18). The hydrolyzed ¹¹C-labeled compound is 2-[1-¹¹C]-butyrylglycerol, which is also able to return to serum, and it is further converted to 1-[1-¹¹C]butyryl-*rac*-glycerol or phosphorylated compounds. On the contrary, ¹¹C activity in the 1-position of 1-[1-¹¹C]butyryl-2-palmitoyl-*rac*-glycerol is readily converted to [1-¹¹C]butyryl CoA and is taken into the TCA cycle, resulting in the production of ¹¹CO₂. The difference in the labeling position between the two isomers should reflect the difference in the tissue-specific metabolic features of ¹¹C-butyryl moiety.

The present findings show that the brain uptake of 1,2-[¹¹C]DAG is due to accumulation of radioactivity based on PI metabolic processes. The finding that the regions with high neuronal activity related to PKC (13,15,33), correspond with those showing high uptake of *sn*-1,2-[¹¹C]-DAG (12) suggests an in vivo linkage between PI turnover and PKC, as anticipated by Nishizuka (4). As shown by the time-activity curve (Fig. 7) obtained using a coincidental gamma counter, the PI turnover rate can be measured by using 1,2-[¹¹C]DAG and a similar measurement with PET may be possible in humans.

ACKNOWLEDGMENT

This work was supported by Grant-in-Aid for Science Research (02454337) from the Ministry of Education Science and Culture of Japan.

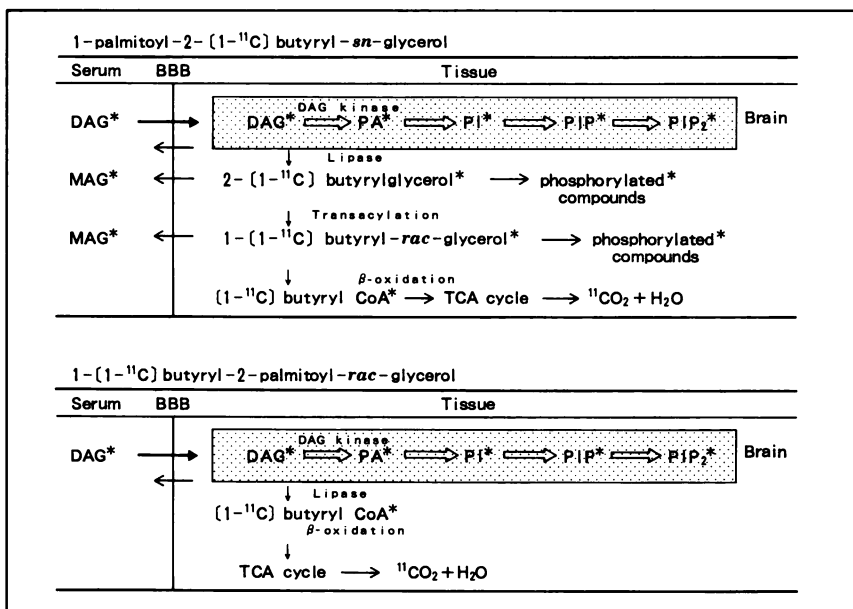


FIGURE 9. Metabolic fates of extrinsic added *sn*- and *rac*-1,2-[¹¹C]DAG. These schematic figures show each metabolic course of *sn*-1,2-[¹¹C]-DAG and *rac*-1,2-[¹¹C]DAG which involved inactive *sn*-2,3-[¹¹C]DAG in the racemic mixture. * indicates each radioactive compound. In rat brain, PI turnover, written as \Rightarrow , should be predominant for both tracers. However, different metabolic fates were demonstrated in other organs due to the predominance in the catabolic course by lipases according to the difference in the ¹¹C labeling position. The shaded frames represent the brain compartment.

REFERENCES

1. Berridge MJ. Inositol trisphosphate and diacylglycerol as second messengers. *Biochem J* 1984;220:345-360.
2. Nishizuka Y. The role of protein kinase C in cell surface signal transduction and tumour promotion. *Nature* 1984;308:693-698.
3. Snider RM, Fisher SK, Agranoff BW. Inositide-linked second messengers in the central nervous system. In: Meltzer HY, ed. *Psychopharmacology: the third generation of progress*. New York: Raven Press; 1987:317-324.
4. Nishizuka Y. Studies and perspectives of protein kinase C. *Science* 1986;233:305-312.
5. Akers RF, Lovinger DM, Colley PA, Linden DJ, Rottnerberg A. Translocation of protein kinase C activity may mediate hippocampal long-term potentiation. *Science* 1986;231:587-589.
6. Olds JL, Anderson ML, McPhie DL, Staten LD, Alon DL. Imaging of memory-specific changes in the distribution of protein kinase C in the hippocampus. *Science* 1989;245:866-869.
7. Imahori Y, Fujii R, Ido T, Hirakawa, Nakahashi H. Phorbol 13-[C-11]-butyrate for the second messenger imaging based on a receptor binding to protein kinase C. *J Cereb Blood Flow Metab* 1989;9(suppl1):s251.
8. Imahori Y, Ido T, Fujii R, et al. C-11-labeled phorbol esters: the specific binding to protein kinase C in vivo by PET [Abstract]. *J Nucl Med* 1989;30:783.
9. Imahori Y, Fujii R, Ido T, Hirakawa K, Nakahashi H. Positron labeled phorbol ester: synthesis method for "non-carrier added" phorbol 13-[1-¹¹C]butyrate using ketene reaction. *J Labelled Compd Radiopharm* 1989;27:1025-1034.
10. Imahori Y, Fujii R, Ido T, et al. Positron labeled sn-1,2-diacylglycerols for the phosphatidylinositol turnover measurement by positron emission tomography [Abstract]. *J Nucl Med* 1990;31:738.
11. Imahori Y, Fujii R, Ido T, et al. Metabolic fates of extrinsic added 1,2-[¹⁴C]diacylglycerols for a phosphatidylinositol turnover measurement by PET [Abstract]. *J Nucl Med* 1991;32:1097.
12. Imahori Y, Fujii R, Ueda S, et al. No-carrier-added carbon-11-labeled sn-1,2- and sn-1,3-diacylglycerols by [¹¹C]propyl ketene method. *J Nucl Med* 1991;32:1622-1626.
13. Nagle DS, and Blumberg PM. Regional localization by light microscopic autoradiography of receptors in mouse brain for phorbol ester tumor promoters. *Cancer Lett* 1983;18:35-40.
14. Murphy KMM, Gould RJ, Oster-Granite ML, Gearhart JD, Snyder SH. Phorbol ester receptors: autoradiographic identification in the developing rat. *Science* 1983;222:1036-1038.
15. Worley PF, Baraban JM, Snyder SH. Heterogeneous localization of protein kinase C in rat brain: autoradiographic analysis of phorbol ester receptor binding. *J Neurosci* 1986;6:199-207.
16. Hajra AK, Fisher SK, Agranoff BW. Isolation, separation, and analysis of phosphoinositides from biological sources. In: Boulton AA, Baker GB, and Horrocks LA eds. *Neuromethods, volume 7: lipids and related compounds*. Clifton, New Jersey: Humana Press, 1988, 211-225.
17. Kanoh H, Åkesson B. Properties of microsomal and soluble diacylglycerol kinase in rat liver. *Eur J Biochem* 1978;85:225-232.
18. Paltauf F, Wagner E. Stereospecificity of lipases. Enzymatic hydrolysis of enantiomeric alkyl diacyl- and dialkylacyl-glycerols by lipoprotein lipase. *Biochim Biophys Acta* 1976;431:359-362.
19. McNamara MJC, Schmitt JD, Wykle RL, Daniel LW. 1-O-hexadecyl-2-acetyl-sn-glycerol stimulates differentiation of HL-60 human promyelocytic leukemia cells to macrophage-like cells. *Biochem Biophys Res Comm* 1984;122:824-830.
20. Fujii R, Imahori Y, Ido T, et al. New synthesis method of [C-11]propyl ketene using HCl/He gas mixture and the reactions on various alcohols. VIII International Symposium on Radiopharmaceutical Chemistry, 1990;123:123-124.
21. Fujii R, Imahori Y, Ido T, et al. New synthesis system of (C-11) propyl ketene and its reactions with various alcohols. *J Labelled Compd Radiopharm* 1991;29:497-505.
22. Zwaal RFA, Roelofsen B, Comfurius P, Van Deenen LLM. Complete purification and some properties of phospholipase C from *Bacillus cereus*. *Biochim Biophys Acta* 1971;233:474-479.
23. Cabot MC, Jaken S. Structural and chemical specificity of diacylglycerols for protein kinase C activation. *Biochem Biophys Res Commun* 1984;125:163-169.
24. Mavis RD, Bell RM, Vagelos PR. Effect of phospholipase C hydrolysis of membrane phospholipids on membranous enzymes. *J Biol Chem* 1972;247:2835-2841.
25. Volpi M, Yassin R, Naccache PH, Sha'afi RI. Chemotactic factor causes rapid decreases in phosphatidylinositol 4,5-bisphosphate and phosphatidylinositol 4-monophosphate in rabbit neutrophils. *Biochem Biophys Res Commun* 1983;112:957-964.
26. DeGeorge JJ, Nariai T, Yamazaki S, Williams WM, Rapoport SI. Arecoline-stimulated brain incorporation of intravenously administered fatty acids in unanesthetized rats. *J Neurochem* 1991;56:352-355.
27. Lapetina EG, Reep B, Ganong BR, Bell RM. Exogenous sn-1,2-diacylglycerols containing saturated fatty acids function as bioregulators of protein kinase C in human platelets. *J Biol Chem* 1985;260:1358-1361.
28. Davis RJ, Ganong BR, Bell RM, Czech MP. sn-1,2-dioctanoyl glycerol: a cell-permeable diacylglycerol that mimics phorbol diester action on the epidermal growth factor receptor and mitogenesis. *J Biol Chem* 1985;260:1562-1566.
29. Faauel J, Chap H, Roques V, S Levy-Toledano, Douste-Blazy L. Biochemical characterization of plasma membranes and inter-cellular membranes isolated from human platelets using Precoil gradients. *Biochim Biophys Acta* 1986;856:155-164.
30. Astrup J. Energy-requiring cell functions in the ischemic brain. *J Neurosurg* 1982;56:482-497.
31. Stephens LR, and Logan SD. Inositol lipid metabolism in rat hippocampal formation slices: basal metabolism and effects of cholinergic agonists. *J Neurochem* 1989;52:179-186.
32. Soukup JF, Friedel RO, Schanberg SM. Cholinergic stimulation of polyphosphoinositide metabolism in brain in vivo. *Biochem Pharmacol* 1978;27:1239-1243.
33. Worley PF, Baraban JM, Snyder SH. Beyond receptors: multiple second-messenger system in brain. *Ann Neurol* 1987;21:217-229.